

The N^3LO Twist-2 Matching of Linearly Polarized Gluon TMDs

Yu Jiao Zhu^a

^a*Max-Planck-Institut für Physik, Werner-Heisenberg-Institut, Boltzmannstr. 8, 85748 Garching, German*

E-mail: yzhu@mpp.mpg.de

ABSTRACT: We compute the twist-2 matching of the transverse-momentum-dependent (TMD) linearly polarized gluon parton distribution and fragmentation functions at next-to-next-to-next-to-leading order (N^3LO) in QCD, supplemented by next-to-next-to-leading logarithmic (NNLL) small- x resummation for the gluon TMD fragmentation functions. These results provide high-precision fixed-order and resummed inputs to TMD phenomenology, and constitute essential theoretical ingredients for future studies of the spin structure and three-dimensional tomography of hadrons at the Electron-Ion Collider (EIC).

Contents

1	Introduction	2
2	Definition of linearly polarized gluon TMD PDFs and FFs	2
3	N^3LO coefficients for linearly polarized gluon TMDs	5
3.1	Renormalization group equations for renormalized coefficient functions	5
3.2	Numerical fits of the $N3LO$ coefficients	7
3.2.1	Numerical fit for TMD PDFs	8
3.2.2	Numerical fit for TMD FFs	10
3.3	Perturbative convergence	12
3.4	$\mathcal{N} = 1$ supersymmetry sum rule for the linearly polarized gluon contribution	13
4	Small x expansion of the TMD coefficients and resummation for the TMD FFs	14
4.1	Small- x expansion of linearly polarized gluon TMD PDFs	14
4.2	Small- z expansion of linearly polarized gluon TMD FFs	15
4.3	Resummation of small- z logarithms for linearly polarized gluon TMD FFs	16
5	Conclusion	18
A	QCD Beta Function	18
B	Anomalous dimension	19
C	Renormalization Constants	20

1 Introduction

The linearly polarized gluon distribution $h_1^{\perp g}$ contributes to observables through quantum interference between left- and right-handed gluon states. While perturbatively suppressed by one order in α_s , the $h_1^{\perp g}$ term induces measurable azimuthal modifications to the shape of the transverse momentum spectrum, which has been studied in phenomenological predictions for diphoton processes [1, 2], vector boson plus jet production [3, 4], dijets or heavy quark pairs productions [5–11], and quarkonium production [12–17]. The linearly polarized gluon TMDs also contribute to Higgs transverse momentum distribution [18–21], thereby enabling precision study of Higgs properties [22]. In contrast, gluon TMD fragmentation function has received much less attention, despite their importance for hadronization dynamics in multi-jet events. The three-point energy correlator in the coplanar limit with one identified hadron can be used to access gluon TMD fragmentation dynamics [23].

Reliable theoretical predictions within the TMD factorization framework require the perturbative matching of TMDs onto collinear PDFs at small b_T . These matching coefficients provide boundary conditions for both analytic resummation and global fits. For the unpolarized gluon distribution f_1^g , the matching is known up to N³LO [24–26]. For the linearly polarized gluon distribution $h_1^{\perp g}$, the NNLO matching coefficients were computed independently in [18, 27]. However, the N³LO matching coefficient for $h_1^{\perp g}$ has remained unknown, representing a key missing ingredient for extending precision predictions.

In this work, we present the first analytic computation of the N³LO twist-2 matching coefficient for the linearly polarized gluon TMDs, obtained with an exponential regulator [28]. In addition, we perform NNLL small- x resummation for the coefficient functions of gluon TMD fragmentation functions. Together, these results provide essential theoretical input for advancing precision TMD physics. In particular, the upcoming Electron-Ion Collider (EIC) will enable clean measurements of azimuthal asymmetries in semi-inclusive DIS, and dijet production, offering a unique opportunity to probe the transverse momentum structure and polarization of gluons inside nucleons with unprecedented accuracy. Our results provide essential theoretical input for such measurements.

2 Definition of linearly polarized gluon TMD PDFs and FFs

The gluon TMD PDFs can be defined in terms of SCET [29–33] collinear fields

$$\mathcal{B}_{g/N}^{\text{bare},\mu\nu}(x, b_\perp) = -xP_+ \int \frac{db^-}{2\pi} e^{-ixb^- P^+} \langle N(P) | \mathcal{A}_{n\perp}^{a,\mu}(0, b^-, b_\perp) \mathcal{A}_{n\perp}^{a,\nu}(0) | N(P) \rangle, \quad (2.1)$$

where $N(P)$ is a hadron state with momentum $P^\mu = (\bar{n} \cdot P)n^\mu/2 = P^+ n^\mu/2$, with $n^\mu = (1, 0, 0, 1)$ and $\bar{n}^\mu = (1, 0, 0, -1)$, and $\mathcal{A}_{n\perp}^{a,\mu}$ is the gauge invariant collinear gluon field with color index a and Lorentz index μ .

For sufficiently small b_\perp , the TMD PDFs in Eq. (2.1) admit operator product expansion onto the usual collinear PDFs,

$$\mathcal{B}_{g/N}^{\text{bare},\mu\nu}(x, b_\perp) = \sum_i \int_x^1 \frac{d\xi}{\xi} \mathcal{I}_{gi}^{\text{bare},\mu\nu}(\xi, b_\perp) \phi_{i/N}^{\text{bare}}(x/\xi) + \text{power corrections}, \quad (2.2)$$

where the summation is over all parton flavors i . The perturbative matching coefficients $\mathcal{I}_{gi}^{\text{bare},\mu\nu}(\xi, b_\perp)$ in Eq. (2.2) are independent of the actual hadron N . The perturbative matching coefficients $\Delta\mathcal{I}_{ij}^{\text{bare}}(\xi, b_\perp)$ in Eq. (2.2) are independent of the hadronic state N , as a result, one can replace the hadron N with a partonic state j and compute the matching coefficients within perturbation theory. By inserting a complete set of n -collinear state $\mathbb{1} = \oint_{X_n} dPS_{X_n} |X_n\rangle \langle X_n|$ into the operator definition, the bare gluon beam function can be computed from splitting amplitudes integrated over collinear phase space

$$\mathcal{I}_{gi}^{\text{bare},\mu\nu}(x, b_\perp, \mu, \nu) = \lim_{\tau \rightarrow 0} \sum_{X_n} dPS_{X_n} e^{-iK_\perp \cdot b_\perp} e^{-b_0 \tau \frac{P \cdot K}{P^+}} \delta(K^+ - (1-x)P^+) \mathbf{P}_{g \leftarrow i}^{\mu\nu} \quad (2.3)$$

where K^μ is the total momentum of $|X_n\rangle$, and dPS_{X_n} is the collinear phase space measure, and $\mathbf{P}_{g \leftarrow i}^{\mu\nu}$ is the spin correlator of the color averaged gluon splitting amplitude

$$\mathbf{P}_{g \leftarrow i}^{\mu\nu} \equiv \mathbf{Sp}_{X_n g_\mu^* \leftarrow i}^* \mathbf{Sp}_{X_n g_\nu^* \leftarrow i} \equiv -x P_+ \langle i | \mathcal{A}_{n\perp}^{a,\mu} | X_n \rangle \langle X_n | \mathcal{A}_{n\perp}^{a,\nu} | i \rangle, \quad (2.4)$$

The integral in Eq. (2.3) is properly defined only with a rapidity cutoff implemented through the exponential rapidity regulator $e^{-b_0 \tau \frac{P \cdot K}{P^+}}$ [28, 34], which effectively restricts the total energies of the collinear radiations by a rapidity scale $\nu = 1/\tau$.

A practically useful way to perform the integration in Eq. (2.3) is to first evaluate the k_\perp -unintegrated beam function [35]

$$\begin{aligned} \tilde{\mathcal{I}}_{g/i}^{\mu\nu}(x, \tilde{K}_\perp) &= \left[\lim_{\tau \rightarrow 0} \frac{2 \int d^d K}{V_{d-2}} e^{-b_0 \tau \frac{P \cdot K}{P^+}} \times \delta(K^+ - P^+(1-x)) \delta(\tilde{K}_\perp^2 - K_\perp^2) \right. \\ &\quad \left. \times \sum_{X_n} dPS_{X_n} \delta^{(d)}(K - \sum_{r \in X_n} k_r) \times \mathbf{P}_{g \leftarrow i}^{\mu\nu}(\{k_r\}) \right] \Big|_{\tau \rightarrow 1/\nu}, \end{aligned} \quad (2.5)$$

and subsequently apply a Fourier transformation to convert from momentum space to impact parameter space

$$\mathcal{I}_{gi}^{\text{bare},\mu\nu}(x, b_\perp, \mu, \nu) = \int \frac{d^{d-2} \tilde{K}_\perp}{|\tilde{K}_\perp^2|^{-\epsilon}} e^{-ib_\perp \cdot \tilde{K}_\perp} \tilde{\mathcal{I}}_{g/i}^{\mu\nu}(x, \tilde{K}_\perp), \quad (2.6)$$

where $d = 4 - 2\epsilon$ is the space-time dimension, $b_0 = 2e^{-2\gamma_E}$ is the inverse of characteristic transverse scale, and $V_d = 2\pi^{d/2}/\Gamma(d/2)$ is the volume of d sphere.

By boost invariance and Lorentz covariance, the polarization structure of the gluon beam function admit the following decomposition

$$\begin{aligned} \mathcal{I}_{gi}^{\text{bare},\mu\nu}(x, b_\perp) &= -\frac{g_\perp^{\mu\nu}}{d-2} \mathcal{I}_{gi}^{\text{bare}}(x, b_T) + \left(\frac{g_\perp^{\mu\nu}}{d-2} + \frac{b_\perp^\mu b_\perp^\nu}{b_T^2} \right) \mathcal{I}'_{gi}^{\text{bare}}(x, b_T) \\ &= -\frac{g_\perp^{\mu\nu}}{d-2} \left[-g_{\perp\sigma\tau} \mathcal{I}_{gi}^{\text{bare},\sigma\tau}(x, b_\perp) \right] \\ &\quad + \left(\frac{g_\perp^{\mu\nu}}{d-2} + \frac{b_\perp^\mu b_\perp^\nu}{b_T^2} \right) \left[\frac{1}{d-3} \left(g_{\perp\sigma\tau} + (d-2) \frac{b_{\perp\sigma} b_{\perp\tau}}{b_T^2} \right) \mathcal{I}_{gi}^{\text{bare},\sigma\tau}(x, b_\perp) \right] \\ \tilde{\mathcal{I}}_{g/i}^{\mu\nu}(x, \tilde{K}_\perp) &= -\frac{g_\perp^{\mu\nu}}{d-2} \left[-g_{\perp\sigma\tau} \tilde{\mathcal{I}}_{g/i}^{\sigma\tau}(x, \tilde{K}_\perp) \right] \end{aligned}$$

$$+ \left(\frac{g_{\perp}^{\mu\nu}}{d-2} + \frac{\tilde{K}_{\perp}^{\mu} \tilde{K}_{\perp}^{\nu}}{\tilde{K}_T^2} \right) \left[\frac{1}{d-3} \left(g_{\perp\sigma\tau} + (d-2) \frac{\tilde{K}_{\perp\sigma} \tilde{K}_{\perp\tau}}{\tilde{K}_T^2} \right) \tilde{\mathcal{I}}_{g/i}^{\sigma\tau}(x, \tilde{K}_{\perp}) \right] \quad (2.7)$$

where $b_T^2 = -b_{\perp}^2 > 0$, $b_T = \sqrt{b_T^2}$ and $\tilde{K}_T^2 = -\tilde{K}_{\perp}^2 > 0$, $\tilde{K}_T = \sqrt{\tilde{K}_T^2}$.

Putting Eq. (2.6) and Eq. (2.7) together, we arrive at

$$\begin{aligned} \mathcal{I}_{gi}^{\text{bare},\mu\nu}(x, b_{\perp}) = & - \frac{g_{\perp}^{\mu\nu}}{d-2} \int \frac{d^{d-2} \tilde{K}_{\perp}}{|\tilde{K}_{\perp}^2|^{-\epsilon}} e^{-ib_{\perp}\cdot\tilde{K}_{\perp}} \left[-g_{\perp\sigma\tau} \tilde{\mathcal{I}}_{g/i}^{\sigma\tau}(x, \tilde{K}_{\perp}) \right] \\ & + \left(\frac{g_{\perp}^{\mu\nu}}{d-2} + \frac{b_{\perp}^{\mu} b_{\perp}^{\nu}}{b_T^2} \right) \int \frac{d^{d-2} \tilde{K}_{\perp}}{|\tilde{K}_{\perp}^2|^{-\epsilon}} e^{-ib_{\perp}\cdot\tilde{K}_{\perp}} \left[\frac{-1 + (d-2)(b_{\perp}\cdot\tilde{K}_{\perp})^2/b_T^2 \tilde{K}_T^2}{(d-3)^2} \right. \\ & \times \left. \left(g_{\perp\sigma\tau} + (d-2) \frac{\tilde{K}_{\perp\sigma} \tilde{K}_{\perp\tau}}{\tilde{K}_T^2} \right) \tilde{\mathcal{I}}_{g/i}^{\sigma\tau}(x, \tilde{K}_{\perp}) \right], \end{aligned} \quad (2.8)$$

and thus

$$\begin{aligned} \mathcal{I}_{gi}^{\text{bare}}(x, b_T) = & \int \frac{d^{d-2} \tilde{K}_{\perp}}{|\tilde{K}_{\perp}^2|^{-\epsilon}} e^{-ib_{\perp}\cdot\tilde{K}_{\perp}} \left[-g_{\perp\sigma\tau} \tilde{\mathcal{I}}_{g/i}^{\sigma\tau}(x, \tilde{K}_{\perp}) \right], \\ \mathcal{I}'_{gi}^{\text{bare}}(x, b_T) = & \int \frac{d^{d-2} \tilde{K}_{\perp}}{|\tilde{K}_{\perp}^2|^{-\epsilon}} e^{-ib_{\perp}\cdot\tilde{K}_{\perp}} \left[\frac{-1 + (d-2)(b_{\perp}\cdot\tilde{K}_{\perp})^2/b_T^2 \tilde{K}_T^2}{(d-3)^2} \right. \\ & \times \left. \left(g_{\perp\sigma\tau} + (d-2) \frac{\tilde{K}_{\perp\sigma} \tilde{K}_{\perp\tau}}{\tilde{K}_T^2} \right) \tilde{\mathcal{I}}_{g/i}^{\sigma\tau}(x, \tilde{K}_{\perp}) \right]. \end{aligned} \quad (2.9)$$

The function $\mathcal{I}_{gi}^{\text{bare}}$ corresponds to the unpolarized gluon distribution and has been discussed extensively in our previous work [26]. The function $\mathcal{I}'_{gi}^{\text{bare}}$ represents the linearly polarized gluon distribution. By tensor decomposition, the corresponding k_{\perp} -unintegrated integrand becomes independent of the external vector b_{\perp} , and therefore the reduction to master integrals proceeds in complete analogy with the unpolarized case [26, 35].

The TMD FFs are defined as crossings of TMD beam functions

$$\mathcal{D}_{N/g}^{\text{bare},\mu\nu}(z, b_{\perp}) = - \frac{P_{\perp}}{z^2} \sum_X \int \frac{db^-}{2\pi} e^{iP^+ b^-/z} \langle 0 | \mathcal{A}_{n\perp}^{a,\mu}(0, b^-, b_{\perp}) | N(P), X \rangle \langle N(P), X | \mathcal{A}_{n\perp}^{a,\nu}(0) | 0 \rangle, \quad (2.10)$$

where $P^{\mu} = (\bar{n} \cdot P)n^{\mu}/2 = P^+ n^{\mu}/2$ is the momenta of the final state detected hadron. According to parton-hardron frame relation [27, 34, 36], performing the calculation in the hadron frame is equivalent to working in the parton frame, but with the argument of the latter replaced by b_{\perp}/z and multiplying the hadron-frame TMDs by a flux factor $z^{2-2\epsilon}$. For convenience, we shall henceforth denote our hadron-frame results as $\mathcal{F}'_{i/g}^{\text{bare}}(z, b_{\perp}/z, \mu, \nu)$.

To obtain the finite coefficient functions, we carry out the proper UV renormalization together with the zero-bin subtraction, which are summarized in the following collinear mass factorization formula

$$\frac{1}{Z_g^B} \frac{\mathcal{I}'_{g/i}^{\text{bare}}(x, b_{\perp}, \mu, \nu)}{\mathcal{S}_{0b}} = \sum_k \mathcal{I}'_{gk}(x, b_{\perp}, \mu, \nu) \otimes \phi_{ki}(x, \mu),$$

$$\frac{1}{Z_g^B} \frac{\mathcal{F}_{i/g}^{\text{bare}}(z, b_\perp/z, \mu, \nu)}{\mathcal{S}_{0\text{b}}} = \sum_k d_{ik}(z, \mu) \otimes \mathcal{C}'_{kg}(z, b_\perp/z, \mu, \nu). \quad (2.11)$$

where $\mathcal{S}_{0\text{b}}(\alpha_s)$ is the bare zero-bin soft function which is the same as the TMD soft function [37], Z_g^B (see in Sec. C) are the multiplicative operator renormalization constants for the gluon correlator, and ϕ_{ki} (d_{ik}) are partonic lightcone PDFs (FFs). \mathcal{I}'_{gi} (\mathcal{C}'_{gi}) is the finite coefficient functions, and is one of the main results for the present work.

3 N³LO coefficients for linearly polarized gluon TMDs

In this section we present our results for coefficient functions \mathcal{I}'_{gi} and \mathcal{C}'_{gi} . We will only show the numeric fit to these functions in the paper, but the full analytic expressions can be found in the ancillary files. For TMD FFs, we give the results for \mathcal{C}_{gi} with an argument b_\perp/z , which after divided by z^2 are exactly the results in the hadron frame.

3.1 Renormalization group equations for renormalized coefficient functions

The renormalized coefficient functions obey the following RG equations

$$\begin{aligned} \frac{d}{d \ln \mu} \mathcal{I}'_{ji}(x, b_\perp, \mu, \nu) &= 2 \left[\Gamma_j^{\text{cusp}}(\alpha_s(\mu)) \ln \frac{\nu}{x P_+} + \gamma_j^B(\alpha_s(\mu)) \right] \mathcal{I}'_{ji}(x, b_\perp, \mu, \nu) \\ &\quad - 2 \sum_k \mathcal{I}'_{jk}(x, b_\perp, \mu, \nu) \otimes P_{ki}(x, \alpha_s(\mu)), \end{aligned} \quad (3.1)$$

$$\begin{aligned} \frac{d}{d \ln \mu} \mathcal{C}'_{ij}(z, b_\perp/z, \mu, \nu) &= 2 \left[\Gamma_j^{\text{cusp}}(\alpha_s(\mu)) \ln \frac{z \nu}{P_+} + \gamma_j^B(\alpha_s(\mu)) \right] \mathcal{C}'_{ij}(z, b_\perp/z, \mu, \nu) \\ &\quad - 2 \sum_k P_{ik}^T(z, \alpha_s(\mu)) \otimes \mathcal{C}'_{kj}(z, b_\perp/z, \mu, \nu). \end{aligned} \quad (3.2)$$

The rapidity evolution equations are [38, 39]

$$\begin{aligned} \frac{d}{d \ln \nu} \mathcal{I}'_{ji}(x, b_\perp, \mu, \nu) &= -2 \left[\int_\mu^{b_0/b_T} \frac{d\bar{\mu}}{\bar{\mu}} \Gamma_j^{\text{cusp}}(\alpha_s(\bar{\mu})) + \gamma_j^R(\alpha_s(b_0/b_T)) \right] \mathcal{I}'_{ji}(x, b_\perp, \mu, \nu), \\ \frac{d}{d \ln \nu} \mathcal{C}'_{ij}(z, b_\perp/z, \mu, \nu) &= -2 \left[\int_\mu^{b_0/b_T} \frac{d\bar{\mu}}{\bar{\mu}} \Gamma_j^{\text{cusp}}(\alpha_s(\bar{\mu})) + \gamma_j^R(\alpha_s(b_0/b_T)) \right] \mathcal{C}'_{ij}(z, b_\perp/z, \mu, \nu). \end{aligned} \quad (3.3)$$

Expanding the perturbative coefficient functions in terms of $\alpha_s/(4\pi)$, the solution to these evolution equations up to $\mathcal{O}(\alpha_s^3)$ reads,

$$\begin{aligned} \mathcal{I}'_{gi}^{(1)}(x, b_\perp, \mu, \nu) &= I'_{gi}^{(1)}, \\ \mathcal{I}'_{gi}^{(2)}(x, b_\perp, \mu, \nu) &= \left[\left(\beta_0 - \frac{1}{2} \Gamma_0^{\text{cusp}} L_Q + \gamma_0^B \right) I'_{gi}^{(1)} - \sum_j I'_{gj}^{(1)} \otimes P_{ji}^{(0)} \right] L_\perp + I'_{gi}^{(2)}, \end{aligned}$$

$$\begin{aligned}
\mathcal{I}_{gi}^{(3)}(x, b_\perp, \mu, \nu) = & \left[\left(-\frac{3}{2}\beta_0 + \frac{1}{2}\Gamma_0^{\text{cusp}} L_Q - \gamma_0^B \right) \sum_j I_{gj}^{'(1)} \otimes P_{ji}^{(0)} + \frac{1}{2} \sum_{jk} I_{gj}^{'(1)} \otimes P_{jk}^{(0)} \otimes P_{ki}^{(0)} \right. \\
& + \frac{1}{8} \left(4\beta_0 + 2\gamma_0^B - \Gamma_0^{\text{cusp}} L_Q \right) \left(2\beta_0 + 2\gamma_0^B - \Gamma_0^{\text{cusp}} L_Q \right) I_{gi}^{'(1)} \Big] L_\perp^2 \\
& + \left[- \sum_j I_{gj}^{'(1)} \otimes P_{ji}^{(1)} - \sum_j I_{gj}^{'(2)} \otimes P_{ji}^{(0)} + \left(2\beta_0 - \frac{1}{2}\Gamma_0^{\text{cusp}} L_Q + \gamma_0^B \right) I_{gi}^{'(2)} \right. \\
& \left. + \left(\beta_1 - \frac{1}{2}\Gamma_1^{\text{cusp}} L_Q + \gamma_1^B \right) I_{gi}^{'(1)} \right] L_\perp + I_{gi}^{'(1)} \gamma_1^R L_Q + I_{gi}^{'(3)}, \tag{3.4}
\end{aligned}$$

where we have used $\gamma_0^R = 0$ to simplify the expression and $I_{gi}^{'(n)}$ are the scale-independent coefficient functions. We have defined

$$L_\perp = \ln \frac{b_T^2 \mu^2}{b_0^2}, \quad L_Q = 2 \ln \frac{x P_+}{\nu}, \quad L_\nu = \ln \frac{\nu^2}{\mu^2}, \quad b_0 = 2e^{-\gamma_E}. \tag{3.5}$$

The matching coefficients of the TMD fragmentation functions allows the following form

$$\begin{aligned}
\mathcal{C}_{ig}^{'(1)}(z, b_\perp/z, \mu, \nu) = & C_{ig}^{'(1)}, \\
\mathcal{C}_{ig}^{'(2)}(z, b_\perp/z, \mu, \nu) = & \left[\left(\beta_0 - \frac{1}{2}\Gamma_0^{\text{cusp}} L_Q + \gamma_0^B \right) C_{ig}^{'(1)} - \sum_j C_{ij}^{'(1)} \otimes P_{jg}^{T(0)} \right] L_\perp + C_{ig}^{'(2)}, \\
\mathcal{C}_{ig}^{'(3)}(z, b_\perp/z, \mu, \nu) = & \left[\left(-\frac{3}{2}\beta_0 + \frac{1}{2}\Gamma_0^{\text{cusp}} L_Q - \gamma_0^B \right) \sum_j C_{ij}^{'(1)} \otimes P_{jg}^{T(0)} + \frac{1}{2} \sum_{jk} C_{ij}^{'(1)} \otimes P_{jk}^{T(0)} \otimes P_{kg}^{T(0)} \right. \\
& + \frac{1}{8} \left(4\beta_0 + 2\gamma_0^B - \Gamma_0^{\text{cusp}} L_Q \right) \left(2\beta_0 + 2\gamma_0^B - \Gamma_0^{\text{cusp}} L_Q \right) C_{ig}^{'(1)} \Big] L_\perp^2 \\
& + \left[- \sum_j C_{ij}^{'(1)} \otimes P_{jg}^{T(1)} - \sum_j C_{ij}^{'(2)} \otimes P_{jg}^{T(0)} + \left(2\beta_0 - \frac{1}{2}\Gamma_0^{\text{cusp}} L_Q + \gamma_0^B \right) C_{ig}^{'(2)} \right. \\
& \left. + \left(\beta_1 - \frac{1}{2}\Gamma_1^{\text{cusp}} L_Q + \gamma_1^B \right) C_{ig}^{'(1)} \right] L_\perp + C_{ig}^{'(1)} \gamma_1^R L_Q + C_{ig}^{'(3)}, \tag{3.6}
\end{aligned}$$

We stress again that due to the chosen argument, the expressions given above are for TMD FFs in the hadron frame. The anomalous dimensions appeared above are identical to those in the space-like case and the scale logarithms are defined as

$$L_\perp = \ln \frac{b_T^2 \mu^2}{b_0^2}, \quad L_Q = 2 \ln \frac{P_+}{z \nu}, \quad L_\nu = \ln \frac{\nu^2}{\mu^2}, \quad b_0 = 2e^{-\gamma_E}, \tag{3.7}$$

Both space-like and time-like coefficient functions depend on the rapidity regulator being used. Rapidity-regulator-independent TMD PDFs and TMD FFs can be obtained by multiplying the coefficient functions with the squared root of the TMD soft functions $\mathcal{S}(b_\perp, \mu, \nu)$ [27, 34]

$$\begin{aligned}
h_{1,gi}^\perp(x, b_\perp, \mu) = & \mathcal{I}_{gi}'(x, b_\perp, \mu, \nu) \sqrt{\mathcal{S}(b_\perp, \mu, \nu)}, \\
h_{1,ig}^{T,\perp}(z, b_\perp/z, \mu) = & \mathcal{C}_{ig}'(z, b_\perp/z, \mu, \nu) \sqrt{\mathcal{S}(b_\perp, \mu, \nu)}. \tag{3.8}
\end{aligned}$$

3.2 Numerical fits of the N3LO coefficients

The coefficient functions develop end-point divergences both in the threshold and high energy limit. We first present here the results for leading threshold limit. The results for high energy limit will be discussed in next section. In the $z \rightarrow 1$ limit, we have

$$\lim_{z \rightarrow 1} \mathcal{I}'_{gg}(z) = \lim_{z \rightarrow 1} \mathcal{C}'_{gg}(z) = 0, \quad (3.9)$$

$$\begin{aligned} \lim_{z \rightarrow 1} \mathcal{I}'^{(1)}_{gg}(z) &= -\lim_{z \rightarrow 1} \mathcal{C}'^{(1)}_{gg}(z) = 0, \\ \lim_{z \rightarrow 1} \mathcal{I}'^{(2)}_{gg}(z) &= -\lim_{z \rightarrow 1} \mathcal{C}'^{(2)}_{gg}(z) = \frac{8}{3} C_A N_f T_F - \frac{4}{3} C_A^2, \\ \lim_{z \rightarrow 1} \mathcal{I}'^{(3)}_{gg}(z) &= -\lim_{z \rightarrow 1} \mathcal{C}'^{(3)}_{gg}(z) = C_A^3 \left(-\frac{68}{9} \ln(1-z) + \frac{4}{3} \zeta_2 - \frac{836}{27} \right) \\ &\quad + C_A^2 N_f T_F \left(\frac{152}{9} \ln(1-z) - \frac{8}{3} \zeta_2 + \frac{2000}{27} \right) \\ &\quad + C_A N_f^2 T_F^2 \left(-\frac{32}{9} \ln(1-z) - \frac{224}{27} \right) - 8 C_A C_F N_f T_F. \end{aligned} \quad (3.10)$$

The analytic expressions for the coefficient functions will be provided in the ancillary files along with the arXiv submission. In this section we will present their numerical fits. Following Ref. [40], we use the following elementary functions to fit the results,

$$L_x \equiv \ln x, L_{\bar{x}} \equiv \ln(1-x), \bar{x} \equiv 1-x. \quad (3.11)$$

We subtract the $x \rightarrow 0$ and $x \rightarrow 1$ limits up to next-to-next-to-leading power (x^1 and $(1-x)^2$) and fit the remaining terms in the region $10^{-6} < x < 1$. The fitted data in the full region $0 < x < 1$ has an accuracy better than 10^{-3} . Below we show the numerical fitting with six significant digits for the scale independent part of the coefficient functions, the full numerical fitting is also attached as ancillary files with the arXiv submission.

3.2.1 Numerical fit for TMD PDFs

The numerical fit for $q \rightarrow g$ channel reads

$$I'_{gq}^{(1)}(x) = -16. - 5.33333x^2 + 16.x + \frac{5.33333}{x} + 5.33333\bar{x}^2 + 5.33333\bar{x}, \quad (3.12)$$

$$\begin{aligned} I'_{gq}^{(2)}(x) = & 60.0576 + x^3 (1.73689L_x^2 + 1.31146L_x + 181.777) \\ & + x^2 (-0.0962441L_x^2 - 1.05262L_x - 485.159) + 24.8889L_x^2 \\ & - 124.444L_x + \frac{-64.L_x - 144.387}{x} + \bar{x}^3 (73.1746L_{\bar{x}} - 3.61139L_{\bar{x}}^2) \\ & + \bar{x}^2 (18.3242L_{\bar{x}}^2 + 109.696L_{\bar{x}} + 80.) + \bar{x} (17.7778L_{\bar{x}}^2 + 39.1111L_{\bar{x}} + 167.111) \\ & - 0.830867x^6 + 1.09121x^5 - 13.0824x^4 + 520.649x + N_f \left(21.3333 - 4.58899\bar{x}^3L_{\bar{x}} \right. \\ & \left. + \bar{x}^2 (-6.97809L_{\bar{x}} - 4.74074) + \bar{x} (-7.11111L_{\bar{x}} - 4.74074) + 0.0858469x^6 \right. \\ & \left. + 0.0306905x^5 + 0.857775x^4 - 10.1641x^3 + 29.0533x^2 - 36.4561x - \frac{4.74074}{x} \right), \end{aligned} \quad (3.13)$$

$$\begin{aligned} I'_{gq}^{(3)}(x) = & x^3 (42.5798L_x^4 - 193.828L_x^3 + 1870.84L_x^2 - 5175.95L_x + 27899.) \\ & + x^2 (-1.39715L_x^4 - 46.3058L_x^3 - 589.57L_x^2 - 3130.51L_x - 57234.9) \\ & + x (-85.9259L_x^3 - 29.037L_x^2 - 496.39L_x + 33967.) - 66.1728L_x^4 \\ & + 675.951L_x^3 - 5327.95L_x^2 + 15498.2L_x + \frac{384.L_x^2 + 6505.91L_x + 23170.5}{x} \\ & + \bar{x}^3 (-171.255L_{\bar{x}}^4 + 427.309L_{\bar{x}}^3 - 4879.47L_{\bar{x}}^2 + 11122.7L_{\bar{x}}) \\ & + \bar{x}^2 (31.6098L_{\bar{x}}^4 + 472.534L_{\bar{x}}^3 + 2793.57L_{\bar{x}}^2 + 12374.5L_{\bar{x}} + 460.455) \\ & + \bar{x} (29.6296L_{\bar{x}}^4 + 195.556L_{\bar{x}}^3 + 1255.65L_{\bar{x}}^2 + 3355.75L_{\bar{x}} + 4895.03) \\ & + 5.57818x^6 + 61.8984x^5 + 1608.03x^4 - 29477.1 \\ & + N_f \left(x^3 (-125.431L_x^4 + 647.745L_x^3 - 6056.05L_x^2 + 17440.5L_x - 33441.6) \right. \\ & \left. + 5.92593L_x^4 + x^2 (5.17351L_x^4 + 159.374L_x^3 + 2027.33L_x^2 + 12536.L_x + 32378.) \right. \\ & \left. - 22.1235L_x^3 + 1890.26 + x (2.37037L_x^3 + 33.7778L_x^2 - 169.679L_x - 1858.54) \right. \\ & \left. + \frac{-47.8311L_x - 770.159}{x} + 1877.86x^4 + \bar{x}^3 (26.4305L_{\bar{x}}^3 - 223.37L_{\bar{x}}^2 + 361.635L_{\bar{x}}) \right. \\ & \left. + 167.506L_x^2 - 245.339L_x + \bar{x}^2 (-26.6999L_{\bar{x}}^3 - 219.428L_{\bar{x}}^2 - 196.645L_{\bar{x}} - 492.978) \right. \\ & \left. + 11.3174x^6 - 87.2009x^5 + \bar{x} (-27.6543L_{\bar{x}}^3 - 139.852L_{\bar{x}}^2 - 419.773L_{\bar{x}} - 746.398) \right) \\ & + N_f^2 \left(\bar{x}^3 (3.13057L_{\bar{x}}^2 + 6.92382L_{\bar{x}}) + \bar{x}^2 (7.30548L_{\bar{x}}^2 + 11.6468L_{\bar{x}} + 10.2716) \right. \\ & \left. + \bar{x} (7.11111L_{\bar{x}}^2 + 9.48148L_{\bar{x}} + 10.2716) - 0.0798005x^6 - 0.264696x^5 - 40.2963 \right. \\ & \left. - 3.35431x^4 + 28.7642x^3 - 65.7595x^2 + 70.7187x + \frac{10.2716}{x} \right). \end{aligned} \quad (3.14)$$

The numerical fit for $g \rightarrow g$ channel reads

$$I'_{gg}^{(1)}(x) = -36. - 12.x^2 + 36.x + \frac{12.}{x} + 12.\bar{x}^2 + 12.\bar{x}, \quad (3.15)$$

$$\begin{aligned} I'_{gg}^{(2)}(x) = & x^3 (59.9902L_x^2 + 25.45L_x + 571.357) + x^2 (-3.90622L_x^2 - 41.48L_x - 833.343) \\ & + 72.L_x^2 - 228.L_x + \frac{-144.L_x - 384.871}{x} + 146.24\bar{x}^3L_{\bar{x}} + \bar{x}^2 (141.37L_{\bar{x}} + 154.) \\ & + 292.\bar{x} + 182.871 - 12.5201x^6 + 43.8218x^5 - 202.96x^4 + 623.644x + N_f \left(33.3333 \right. \\ & \left. - 5.33333L_x^2 - 8.L_x + 13.3333x^2 - 30.6667x - \frac{12.}{x} - 22.6667\bar{x}^2 - 21.3333\bar{x} \right), \end{aligned} \quad (3.16)$$

$$\begin{aligned} I'_{gg}^{(3)}(x) = & N_f^2 \left(-15.4325 + x^3 (0.720139L_x^2 - 2.65876L_x + 8.87839) \right. \\ & + x^2 (-2.39953L_x^2 - 9.48416L_x - 34.4843) + x (7.11111L_x^2 + 27.1111L_x + 12.532) \\ & + 11.8519L_x^2 + 41.1724L_x + 0.557351\bar{x}^3L_{\bar{x}} + \bar{x}^2 (13.0983L_{\bar{x}} + 23.8084) - 2.66667L_{\bar{x}} \\ & \left. + \bar{x} (2.66667L_{\bar{x}} + 29.9259) - 0.0575741x^6 + 0.19494x^5 - 0.96427x^4 + \frac{23.1111}{x} \right) \\ & + N_f \left(5230.34 + x^3 (-80.3575L_x^4 + 304.816L_x^3 - 3472.9L_x^2 + 8942.15L_x - 18111.9) \right. \\ & + x^2 (2.35664L_x^4 + 73.9843L_x^3 + 964.128L_x^2 + 6267.36L_x + 18142.2) \\ & + x (15.7037L_x^3 + 317.185L_x^2 + 731.626L_x - 4550.5) + 23.7037L_x^4 - 47.7037L_x^3 \\ & - 55.9519x^5 + 1290.47x^4 + 804.964L_x^2 + 212.774L_x + \frac{-94.2867L_x - 1648.92}{x} \\ & + \bar{x} (97.3333L_{\bar{x}} - 1739.06) + 1.845x^6 + \bar{x}^3 (24.5475L_{\bar{x}}^3 + 16.4844L_{\bar{x}}^2 + 13.5722L_{\bar{x}}) \\ & \left. + \bar{x}^2 (3.17914L_{\bar{x}}^3 - 56.1555L_{\bar{x}}^2 - 340.641L_{\bar{x}} - 1231.01) + 76.L_{\bar{x}} \right) - 75008.4 \\ & + x^3 (5048.8L_x^4 - 20460.3L_x^3 + 220891.L_x^2 - 563699.L_x + 1.15243 \times 10^6) \\ & + x^2 (-146.656L_x^4 - 4774.47L_x^3 - 63544.1L_x^2 - 405209.L_x - 1.07734 \times 10^6) \\ & + x (-360.L_x^3 - 1890.L_x^2 - 7070.08L_x + 32169.) - 180.L_x^4 + 1356.L_x^3 \\ & - 14587.1L_x^2 + 31973.9L_x + \frac{864.L_x^2 + 15358.3L_x + 55590.9}{x} \\ & + \bar{x}^3 (893.277L_{\bar{x}}^2 + 4458.05L_{\bar{x}}) + \bar{x}^2 (602.402L_{\bar{x}}^2 + 5880.86L_{\bar{x}} + 3162.92) \\ & - 204.L_{\bar{x}} + \bar{x} (535.02L_{\bar{x}} + 6512.19) - 583.156x^6 + 5104.62x^5 - 93142.7x^4, \end{aligned} \quad (3.17)$$

3.2.2 Numerical fit for TMD FFs

Similar to Eq. (3.11), for the TMDFFs data we define

$$L_z \equiv \ln z, L_{\bar{z}} \equiv \ln(1-z), \bar{z} \equiv 1-z. \quad (3.18)$$

The numerical fit for $g \rightarrow q$ channel reads

$$C'_{qg}^{(1)}(z) = 2.\bar{z}^2 - 2.\bar{z} \quad (3.19)$$

$$\begin{aligned} C'_{qg}^{(2)}(z) = N_f & \left(z(5.33333 - 2.66667L_z) + \bar{z}^2(0.888889 - 2.66667L_{\bar{z}}) \right. \\ & + z^2(2.66667L_z - 2.66667) + \bar{z}(2.66667L_{\bar{z}} + 1.77778) - 2.66667 \\ & + z^3(0.218193L_z^2 - 3.2449L_z - 3.90061) + z^2(7.99543L_z^2 - 54.7234L_z + 1.46858) \\ & + z(44.L_z^2 + 96.L_z - 38.119) + 6.66667L_z + \bar{z}^3(0.308136L_{\bar{z}}^2 - 4.31322L_{\bar{z}}) \\ & + \bar{z}^2(6.65962L_{\bar{z}}^2 + 25.2474L_{\bar{z}} - 45.7974) + \bar{z}(-6.66667L_{\bar{z}}^2 - 14.6667L_{\bar{z}} + 3.1307) \\ & \left. + 0.0267835z^6 - 0.0724324z^5 + 0.596675z^4 + 40. \right), \end{aligned} \quad (3.20)$$

$$\begin{aligned} C'_{qg}^{(3)}(z) = N_f & \left(z^3(-49.5407L_z^4 + 291.12L_z^3 - 2550.05L_z^2 + 7675.49L_z - 14579.3) \right. \\ & + z^2(2.40456L_z^4 + 62.6266L_z^3 + 848.657L_z^2 + 5730.18L_z + 14183.9) \\ & + z(8.44444L_z^4 + 20.4444L_z^3 + 50.8148L_z^2 - 395.578L_z - 157.261) + 2.8226z^6 \\ & - 29.8543z^5 + 646.547z^4 + \frac{-4.74074L_z^2 - 2.5679L_z + 1.06851}{z} - 67.884 \\ & - 9.77778L_z^3 + 6.88889L_z^2 + 67.1852L_z + \bar{z}^3(-1.16164L_{\bar{z}}^3 + 6.99385L_{\bar{z}}^2 - 96.4745L_{\bar{z}}) \\ & + \bar{z}^2(-10.4184L_{\bar{z}}^3 - 60.3494L_{\bar{z}}^2 + 77.2186L_{\bar{z}} + 227.808) \\ & + \bar{z}(10.3704L_{\bar{z}}^3 + 52.4444L_{\bar{z}}^2 + 25.8201L_{\bar{z}} - 40.7011) \Big) + 1162.44 \\ & + N_f^2 \left(3.55556 - 0.352232z^4 + z^3(-0.1504L_z^2 + 2.15947L_z + 0.627923) \right. \\ & + z^2(2.66999L_z^2 - 8.8481L_z + 6.38239) + z(-2.66667L_z^2 + 3.55556L_z - 10.2442) \\ & + \bar{z}^3(2.15946L_{\bar{z}} - 0.150376L_{\bar{z}}^2) + \bar{z}^2(2.66999L_{\bar{z}}^2 - 1.73701L_{\bar{z}} - 8.47669) \\ & + \bar{z}(-2.66667L_{\bar{z}}^2 - 3.55556L_{\bar{z}} + 4.92113) - 0.0153031z^6 + 0.0459082z^5 \Big) \\ & + z^3(-45.1957L_z^4 + 36.1904L_z^3 - 1438.77L_z^2 + 3275.74L_z - 8151.69) \\ & + z^2(-50.0147L_z^4 + 445.763L_z^3 - 883.432L_z^2 + 5336.81L_z + 7361.47) \\ & + z(-323.333L_z^4 - 1464.15L_z^3 - 3094.22L_z^2 + 361.681L_z - 820.487) \\ & + 57.8519L_z^3 - 31.6667L_z^2 - 229.142L_z + \frac{32.L_z^2 + 10.6667L_z - 4.}{z} \\ & + \bar{z}^3(18.863L_{\bar{z}}^4 - 82.0146L_{\bar{z}}^3 + 736.555L_{\bar{z}}^2 - 1157.05L_{\bar{z}}) \\ & + \bar{z}^2(10.6961L_{\bar{z}}^4 + 91.4333L_{\bar{z}}^3 + 38.4208L_{\bar{z}}^2 - 1814.23L_{\bar{z}} - 2552.26) \\ & + \bar{z}(-11.1111L_{\bar{z}}^4 - 73.3333L_{\bar{z}}^3 - 251.545L_{\bar{z}}^2 - 52.1219L_{\bar{z}} + 747.919) \\ & \left. - 7.34191z^6 - 1.52477z^5 + 461.132z^4 \right), \end{aligned} \quad (3.21)$$

The numerical fit for $g \rightarrow g$ channel reads

$$C_{gg}'^{(1)}(z) = 12.\bar{z} - 12.\bar{z}^2, \quad (3.22)$$

$$\begin{aligned} C_{gg}'^{(2)}(z) = & -42. + z^3 (-0.859465L_z^2 + 119.525L_z - 75.5526) \\ & + z^2 (71.7016L_z^2 - 146.862L_z + 1123.6) + z (-432.L_z^2 - 804.L_z - 953.206) \\ & - 144.L_z + \frac{48.L_z - 4.}{z} + 63.9862\bar{z}^3L_{\bar{z}} + \bar{z}^2 (-144.325L_{\bar{z}} - 298.) - 2.21135z^6 \\ & + 7.79947z^5 - 42.4337z^4 + 280.\bar{z} + N_f \left(6.66667 + z (16.L_z^2 + 24.L_z + 17.3333) \right. \\ & \left. + 21.3333L_z + \frac{-7.11111L_z - 0.148148}{z} - 27.8519z^2 + 17.3333\bar{z}^2 - 17.3333\bar{z} \right), \end{aligned} \quad (3.23)$$

$$\begin{aligned} C_{gg}'^{(3)}(z) = & N_f^2 \left(-25.2286 + z^3 (-18.1777L_z^3 + 24.3323L_z^2 - 298.898L_z + 212.883) \right. \\ & + z^2 (-0.811839L_z^3 - 21.1239L_z^2 - 132.408L_z - 235.919) \\ & + z (9.48148L_z^3 - 19.5556L_z^2 - 36.9502L_z - 45.6169) - 47.4074L_z \\ & + \frac{6.32099L_z + 0.72428}{z} - 11.079z^3L_{\bar{z}} + \bar{z}^2 (-5.88457L_{\bar{z}} - 21.2899) + 2.66667L_{\bar{z}} \\ & + 1.84883z^6 - 12.3415z^5 + 109.871z^4 + 26.3704\bar{z} \Big) + N_f \left(-2142.97 \right. \\ & + z^3 (-210.187L_z^4 + 1087.21L_z^3 - 10056.2L_z^2 + 29048.7L_z - 55575.) \\ & + z^2 (8.74604L_z^4 + 358.925L_z^3 + 2898.99L_z^2 + 21674.2L_z + 52111.4) \\ & + z (-192.593L_z^4 - 381.333L_z^3 - 356.028L_z^2 - 1500.86L_z + 2387.91) + 149.926L_z^3 \\ & + 60.L_z^2 + 217.119L_z + \frac{71.1111L_z^3 + 225.778L_z^2 - 520.309L_z + 76.5496}{z} \\ & + \bar{z}^3 (-4.88908L_{\bar{z}}^3 - 22.3845L_{\bar{z}}^2 - 16.1436L_{\bar{z}}) \\ & + \bar{z}^2 (-3.08125L_{\bar{z}}^3 + 49.9103L_{\bar{z}}^2 + 405.367L_{\bar{z}} + 998.7) - 76.L_{\bar{z}} \\ & + \bar{z} (173.333L_{\bar{z}} - 1421.47) + 10.8466z^6 - 127.723z^5 + 2961.39z^4 \Big) + 11192.3 \\ & + z^3 (3639.81L_z^4 - 23493.5L_z^3 + 188010.L_z^2 - 579411.L_z + 1.05992 \times 10^6) \\ & + z^2 (-393.642L_z^4 - 6757.5L_z^3 - 58150.6L_z^2 - 414850.L_z - 1.07276 \times 10^6) \\ & + z (3528.L_z^4 + 14100.L_z^3 + 27418.6L_z^2 + 65844.1L_z + 40710.2) - 792.L_z^3 \\ & - 558.L_z^2 - 661.554L_z + \frac{-480.L_z^3 - 1464.L_z^2 + 2438.26L_z - 681.464}{z} \\ & + \bar{z}^3 (889.79L_{\bar{z}}^2 - 666.606L_{\bar{z}}) + \bar{z}^2 (-569.928L_{\bar{z}}^2 - 5480.68L_{\bar{z}} - 1374.39) \\ & + 204.L_{\bar{z}} + \bar{z} (331.02L_{\bar{z}} + 5651.41) - 189.737z^6 + 1817.03z^5 - 39239.z^4, \end{aligned} \quad (3.24)$$

3.3 Perturbative convergence

To investigate the perturbative convergence of (the perturbative part of) the linearly polarized gluon TMD PDF, we consider its first moment

$$h_{1,g/N}^\perp(x, q_T^{\max}) = \sum_i \int_0^{q_T^{\max}} dq_T \int_x^1 \frac{d\xi}{\xi} h_{1,gi}^\perp(\xi, q_T, \mu) \phi_{i/N}(x/\xi, \mu), \quad (3.25)$$

where $h_{1,gi}^\perp(\xi, q_T, \mu)$ are physical TMD coefficients in momentum-space, and q_T^{\max} is a UV cutoff, below which the twist-2 approximation can be justified. In Fig. (1) we plot $xh_{1,g/N}^\perp$ using PDF set NNPDF30_nnlo_as_0118 [41]. We observe the perturbative uncertainties are well under control once higher-order corrections are included, for large enough momentum fraction x ($x > 10^{-3}$). For extremely small x , however, resummation effects becomes important. In particular, the leading-logarithmic (LL) resummed prediction for the coefficient functions was obtained in Ref. [42].

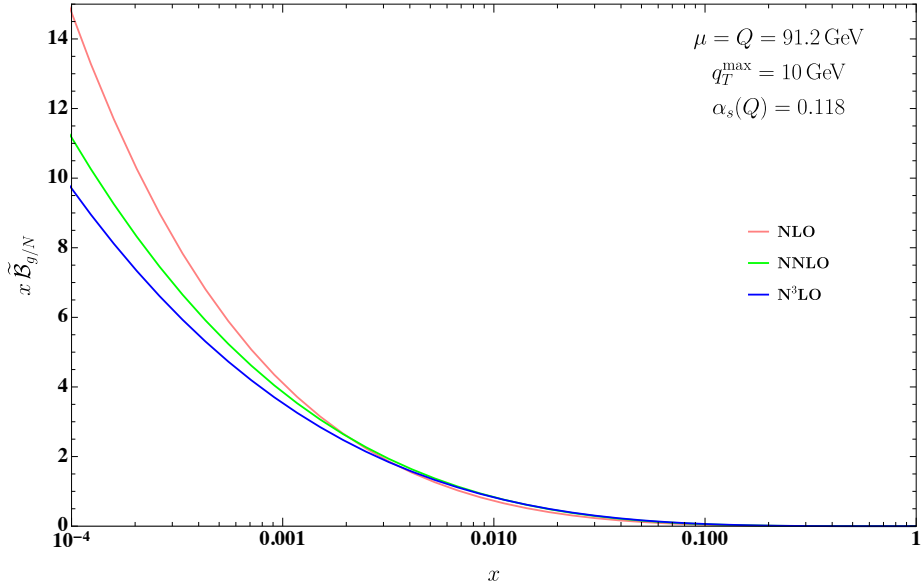


Figure 1. Integrated linearly polarized gluon TMD PDFs at various perturbative order.

As an application of our results, we consider the small transverse momentum (p_T) distributions of Higgs bosons at hadron colliders, using the frameworks of soft-collinear effective theory (SCET) [29–33]. At small $p_T \ll m_H = 125 \text{ GeV}$, the p_T distribution $d\sigma/dp_T^2$ of the produced Higgs bosons factorizes as an product of gluon TMD distributions and $gg \rightarrow H$ hard functions

$$\begin{aligned} d\sigma/dp_T^2 = & \pi\sigma_0 \int dx_a dx_b \delta(x_a x_b - \frac{m_H^2}{s}) \int \frac{d^2\vec{b}}{(2\pi)^2} e^{i\vec{p}_T \cdot \vec{b}} H(m_H, \mu_F) \\ & \times S_\perp(\vec{b}, \mu_F, \nu) \prod_{j=a,b} \mathcal{B}_{g/N_j}^{\alpha\beta}(x_j, \vec{b}, m_H, \mu_F, \nu), \end{aligned} \quad (3.26)$$

where $H(m_H, \mu_F)$ is the IR-finite function for the hard scattering $gg \rightarrow H$ [43–45] and σ_0 is the corresponding born level cross section. We consider the cumulant of the above

factorization formula by introducing a small p_T cut and define the integrated distribution as $\sigma(p_T) = \int_0^{p_T} d\sigma$, the resulting cross section has a large scale logarithm $\ln(p_T^2/m_H^2)$. The helicity density matrices for the unpolarized and linearly polarized gluon distribution are orthogonal to each other, as a result, the factorization formula in Eq. (3.26) can be schematically written as

$$d\sigma/dp_T^2 = \frac{\pi}{2}\sigma_0 H(m_H, \mu_F) \left(h_{1,g}^\perp \otimes h_{1,g}^\perp(p_T, \mu, m_H^2/s) + f_{1,g} \otimes f_{1,g}(p_T, \mu, m_H^2/s) \right). \quad (3.27)$$

where the first term $h_{1,g}^\perp(p_T, \mu_F)^2$ represents linearly polarized gluon contributions, and the second term $f_{1,g}(p_T, \mu)^2$ corresponds to unpolarized gluon contributions. In what follows, we will be particularly concerned with high-order corrections to the former one. To this end, we calculate the contribution of linearly polarized gluons to the integrated small p_T cross section in Eq. (3.3), the renormalization and factorization scales μ_R and μ_F are chosen at typical values with $\mu_R = \mu_F = \kappa m_H$ where $\kappa \in \{0.5, 1, 2\}$.

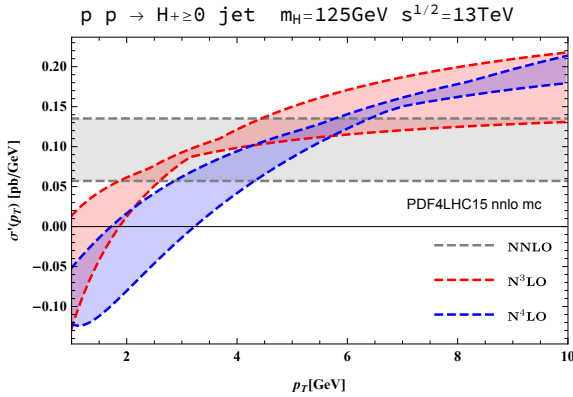


Figure 2. Linearly polarized gluon contributions to the cumulative small p_T cross section, plotted as functions of the artificial cut p_T .

3.4 $\mathcal{N} = 1$ supersymmetry sum rule for the linearly polarized gluon contribution

At two-loop, it was observed that the linearly polarized gluon distribution obeys an momentum conservation sum rule in the $\mathcal{N} = 1$ supersymmetric limit [27]. Our explicit calculations confirms that this sum rule continues to hold at three-loop. Indeed, by setting $C_A = C_F = N_f$ and $T_F = 1/2$ in our perturbative bata, we find that the following sum rule is satisfied

$$\int_0^1 dx x \left(\mathcal{I}'_{gg}(x, b_\perp, \mu, \nu) - \mathcal{I}'_{gq}(x, b_\perp, \mu, \nu) \right) \Big|_{C_F=C_A=N_f} = 0. \quad (3.28)$$

To show the data explicitly, we have

$$\begin{aligned} \left(\mathcal{I}'_{gg}(x, b_\perp, \mu, \nu) - \mathcal{I}'_{gq}(x, b_\perp, \mu, \nu) \right) \Big|_{C_F=C_A=N_f} &= \left(\frac{\alpha_s}{4\pi} C_A \right)^2 \left[-8H_0 - \frac{8(1-x)(x^2-2x-1)}{3x} \right] \\ &+ \left(\frac{\alpha_s}{4\pi} C_A \right)^3 \left[L_\perp \left(L_Q \left(\frac{16}{3x} H_0 + \frac{16(x-1)(x^2-2x-1)}{3x} \right) \right) \right. \\ &\quad \left. - \frac{16}{3x} H_0 \left(\frac{16}{3x} H_0 + \frac{16(x-1)(x^2-2x-1)}{3x} \right) \right] \end{aligned}$$

$$\begin{aligned}
& -\frac{32(x-1)(x^2-2x-1)}{3x}H_1 - \frac{8(4x^3-12x^2+19x+4)}{3x}H_0 \\
& -32H_2 + 16H_{0,0} - \frac{8(x-1)(22x^2-17x-65)}{9x} + 32\zeta_2 \Big) \\
& -\frac{8(x-1)(5x^2-25x-34)}{9x}H_1 + \frac{16(x+1)(x^2+2x-2)}{3x}H_{-1,0} \\
& -\frac{4}{3}(4x^2-18x+9)H_{0,0} - \frac{16(x-1)(x^2-2x-1)}{3x}H_{1,0} \\
& + \left(48\zeta_2 - \frac{4(78x^3-72x^2-109x-30)}{9x} \right) H_0 - \frac{16(x^3-3x^2+7x+4)}{3x}H_2 \\
& -48H_3 + 16H_{-2,0} - 16H_{2,0} + 24H_{0,0,0} + \frac{16(x^3+7x+2)}{3x}\zeta_2 \\
& + \frac{2(x-1)(30x^2+15x-202)}{9x} + 40\zeta_3 \Big], \tag{3.29}
\end{aligned}$$

substituting this into Eq. (3.28), we indeed verify that the expression vanishes. which provides strong check to our three-loop results.

4 Small x expansion of the TMD coefficients and resummation for the TMD FFs

4.1 Small- x expansion of linearly polarized gluon TMD PDFs

Using the analytic expression obtained, we can straightforwardly to obtain the small- x expansion. We find that the LL prediction of Ref. [42] is in agreement with our results. To leading power in the expansion, our results are

$$\begin{aligned}
xI'_{gq}^{(1)}(x) &= C_F, \\
xI'_{gq}^{(2)}(x) &= C_A C_F \left[-16 \ln x - 16\zeta_2 - \frac{88}{9} \right] - \frac{64}{9} C_F N_f T_F, \\
xI'_{gq}^{(3)}(x) &= C_A^2 C_F \left[\left(\frac{16}{3}\zeta_2 - 32\zeta_3 + \frac{15440}{27} \right) \ln x + 32 \ln^2 x - 432\zeta_2 - 400\zeta_3 + 140\zeta_4 + \frac{246713}{81} \right] \\
& + C_A C_F^2 \left[-80\zeta_2 + 120\zeta_3 - 216\zeta_4 + 7 \right] + C_A C_F N_f T_F \left[\left(\frac{256}{3} - \frac{64}{3}\zeta_2 \right) \ln x + \frac{448}{9}\zeta_2 \right. \\
& \left. - 96\zeta_3 - \frac{1048}{81} \right] + C_F^3 \left[16\zeta_2 - 176\zeta_3 + 256\zeta_4 + 10 \right] + C_F^2 N_f T_F \left[\left(\frac{128}{3}\zeta_2 - \frac{6400}{27} \right) \ln x \right. \\
& \left. + \frac{1088}{9}\zeta_2 + 192\zeta_3 - \frac{10724}{9} \right] + \frac{832}{27} C_F N_f^2 T_F^2, \tag{4.1}
\end{aligned}$$

$$\begin{aligned}
xI'_{gg}^{(1)}(x) &= 4C_A, \\
xI'_{gg}^{(2)}(x) &= C_A^2 \left[-16 \ln x - 16\zeta_2 - \frac{148}{9} \right] - \frac{136}{9} C_A N_f T_F + 16C_F N_f T_F, \\
xI'_{gg}^{(3)}(x) &= C_A^3 \left[\left(\frac{16}{3}\zeta_2 - 32\zeta_3 + \frac{16160}{27} \right) \ln x + 32 \ln^2 x - \frac{4288}{9}\zeta_2 - \frac{1432}{3}\zeta_3 + 180\zeta_4 + \frac{260950}{81} \right]
\end{aligned}$$

$$\begin{aligned}
& + C_A^2 N_f T_F \left[\left(112 - \frac{64}{3} \zeta_2 \right) \ln x + \frac{256}{9} \zeta_2 - \frac{160}{3} \zeta_3 + \frac{15632}{81} \right] + C_F^2 N_f T_F \left[\frac{128}{3} \zeta_3 + \frac{8}{3} \right] \\
& + C_A C_F N_f T_F \left[\left(\frac{128}{3} \zeta_2 - \frac{7840}{27} \right) \ln x + \frac{1120}{9} \zeta_2 + \frac{448}{3} \zeta_3 - \frac{131860}{81} \right] + \frac{832}{27} C_A N_f^2 T_F^2.
\end{aligned} \tag{4.2}$$

4.2 Small- z expansion of linearly polarized gluon TMD FFs

To facilitate small- z resummation for TMD FFs, we shall consider the coefficient functions in flavor singlet sector. The flavor singlet (denoted by a superscript s) coefficient functions are written in vector form,

$$\hat{C}^s(z) = \begin{pmatrix} 2N_f C'_{qg}(z) \\ C'_{gg}(z) \end{pmatrix}, \tag{4.3}$$

where $C'_{ig}(z)$ are scaleless coefficient functions as appeared in the RG solutions (3.6).

In contrast to TMD PDFs, which generate a single logarithm at each perturbative order in the small- x limit, TMD FFs in the singlet sector develop double logarithms in the small- z region

$$\lim_{z \rightarrow 0} z \hat{C}_{ig}^s(z) = \lim_{z \rightarrow 0} z \sum_{n=1}^{\infty} a_s^n \hat{C}_{ig}^{s(n)}(z) \sim \sum_{n=1}^{\infty} a_s^n \left(\sum_{m=1}^{2n-2} \ln^{2n-2-m} z \right), \tag{4.4}$$

where $a_s = \alpha_s/(4\pi)$ is our perturbative expansion parameter. The small- z data in the singlet sector reads

$$\begin{aligned}
z \hat{C}_{qg}^{s(1)}(z) &= z \hat{C}_{qg}^{s(2)}(z) = 0, \\
z \hat{C}_{qg}^{s(3)}(z) &= 2N_f C_A^2 T_F \left[\frac{64}{9} \ln^2 z + \frac{64}{27} \ln z - \frac{8}{9} \right] + 2N_f C_A N_f T_F^2 \left[-\frac{64}{27} \ln z - \frac{64}{9} \zeta_2 + \frac{1040}{81} \right] \\
&\quad + 2N_f C_F N_f T_F^2 \left[-\frac{128}{9} \ln^2 z - \frac{64}{27} \ln z + \frac{64}{9} \zeta_2 - \frac{896}{81} \right], \\
z \hat{C}_{gg}^{s(1)}(z) &= 0, \\
z \hat{C}_{gg}^{s(2)}(z) &= C_A^2 \left[\frac{16}{3} \ln z - \frac{4}{9} \right] + C_F N_f T_F \left[\frac{16}{9} - \frac{32}{3} \ln z \right] - \frac{8}{9} C_A N_f T_F, \\
z \hat{C}_{gg}^{s(3)}(z) &= C_A^3 \left[\left(\frac{2912}{27} - \frac{32}{3} \zeta_2 \right) \ln z - \frac{160}{9} \ln^3 z - \frac{488}{9} \ln^2 z + 8\zeta_2 - \frac{128}{3} \zeta_3 + \frac{116}{9} \right] \\
&\quad + C_A^2 N_f T_F \left[\left(\frac{64}{3} \zeta_2 - \frac{2000}{27} \right) \ln z + \frac{32}{9} \ln^2 z + \frac{784}{9} \zeta_2 + \frac{160}{3} \zeta_3 - \frac{17216}{81} \right] \\
&\quad + C_A C_F N_f T_F \left[\frac{320}{9} \ln^3 z + \frac{944}{9} \ln^2 z - \frac{560}{3} \ln z - \frac{928}{9} \zeta_2 - \frac{32}{3} \zeta_3 + 232 \right] + \frac{704}{81} C_A N_f^2 T_F^2 \\
&\quad + C_F^2 N_f T_F \left[32 \ln z + \frac{128}{3} \zeta_3 - \frac{152}{3} \right] + C_F N_f^2 T_F^2 \left[\frac{512}{27} \ln z - \frac{1408}{81} \right],
\end{aligned} \tag{4.5}$$

We note that while both \hat{C}_{qg}^s and \hat{C}_{gg}^s has double logarithmic divergence in the small- z limit, the power of leading logarithmic terms of \hat{C}_{qg}^s is lower by 1 compared to the corresponding leading logarithmic terms of \hat{C}_{gg}^s .

4.3 Resummation of small- z logarithms for linearly polarized gluon TMD FFs

In this subsection, we derive the all-order resummation at NNLL accuracy (resummation of the three highest logarithms) in Eq. (4.4), following the approach proposed in [46] and employing the routines developed in our previous work.

To this end, we start from the collinear factorization formula in Eq. (2.11) for singlet TMD FFs (see (4.3) for the definition of singlet combination)

$$\mathcal{F}_{i/g}^s(z, \epsilon) = \frac{1}{Z_j^B} \frac{\mathcal{F}_{i/g}^{s, \text{bare}}(z, \epsilon)}{\mathcal{S}_{0\text{b}}} = \sum_k d_{ik}^s \otimes C_{kg}^s(z, \epsilon), \quad (4.6)$$

where $\mathcal{F}_{i/j}^s(z, \epsilon)$ is the unfactorized TMD fragmentation function, on which the usual strong coupling renormalization, zero-bin subtraction and operator renormalization have already been performed, while the collinear mass factorization onto the lightcone FFs has not yet been applied. It's also reasonable to drop out all the scale-independent terms in Eq. (4.6), since by RG solutions Eq. (3.6), they depend on lower-order quantities and the splitting functions.

It proves convenient to work in Mellin- N space

$$\mathcal{F}(\bar{N}, \epsilon) = M[\mathcal{F}(z, \epsilon)] := \int_0^1 dz z^{N-1} \mathcal{F}(z, \epsilon), \quad (4.7)$$

where $\bar{N} = N - 1$. Small- z logarithms becomes poles in \bar{N} under Mellin transformation,

$$M\left[\frac{1}{z} \ln^k z\right] \equiv \int_0^1 dz z^{N-1} \frac{1}{z} \ln^k z = \frac{(-1)^k k!}{(N-1)^{k+1}} = \frac{(-1)^k k!}{\bar{N}^{k+1}}. \quad (4.8)$$

In Mellin space the collinear factorization formula Eq. (4.6) becomes

$$\begin{pmatrix} \mathcal{F}_{qg}^s(\bar{N}, \epsilon) \\ \mathcal{F}_{gg}^s(\bar{N}, \epsilon) \end{pmatrix} = \hat{d}^s(\bar{N}, \epsilon) \cdot \begin{pmatrix} \hat{C}_{qg}^s(\bar{N}, \epsilon) \\ \hat{C}_{gg}^s(\bar{N}, \epsilon) \end{pmatrix}, \quad (4.9)$$

where

$$\hat{d}^s(\bar{N}, \epsilon) = \begin{pmatrix} \hat{d}_{qg}^s(\bar{N}, \epsilon) & \hat{d}_{gg}^s(\bar{N}, \epsilon) \\ \hat{d}_{gg}^s(\bar{N}, \epsilon) & \hat{d}_{gg}^s(\bar{N}, \epsilon) \end{pmatrix} \quad (4.10)$$

are the partonic collinear FFs in $\overline{\text{MS}}$ scheme, which evolve with the time-like splitting functions $\hat{\gamma}^T(\bar{N})$

$$\frac{d}{d \ln \mu^2} \hat{d}^s(\bar{N}, \epsilon) = 2 \hat{d}^s(\bar{N}, \epsilon) \cdot \hat{\gamma}^T(\bar{N}). \quad (4.11)$$

The complete NNLO results for $\hat{\gamma}^T(\bar{N})$ can be found in [47], see also [48–50].

The crucial observation of [46] is that unrenormalized collinear functions in dimensional regularization have specific asymptotic behavior in the small- z limit. In the case of TMD FFs, we can write down an general ansatz at small z ,

$$\mathcal{F}_{g/g}^{s(n)}(z, \epsilon) = \frac{1}{\epsilon^{2n-3}} \sum_{l=0}^{n-2} z^{-1-2(n-1-l)\epsilon} \left(\underbrace{c_{gg}^{(1,l,n)}}_{\text{LL}} + \underbrace{\epsilon c_{gg}^{(2,l,n)}}_{\text{NLL}} + \underbrace{\epsilon^2 c_{gg}^{(3,l,n)}}_{\text{NNLL}} + \dots \right),$$

$$\mathcal{F}_{q/g}^{s(n)}(z, \epsilon) = \frac{1}{\epsilon^{2n-4}} \sum_{l=0}^{n-3} z^{-1-2(n-1-l)\epsilon} \left(\underbrace{c_{qg}^{(1,l,n)}}_{\text{LL}} + \underbrace{\epsilon c_{qg}^{(2,l,n)}}_{\text{NLL}} + \underbrace{\epsilon^2 c_{qg}^{(3,l,n)}}_{\text{NNLL}} + \dots \right), \quad (4.12)$$

where $c_{qg}^{(1,l,n)}$ is the leading term in the ϵ expansion and small- z expansion, whose knowledge correspond to LL resummation as labeled in (4.12), and similarly for other terms. Precisely, for $\hat{C}_{gg}^s(z)$ the LL series correspond to $\alpha_s^n \ln^{2n-3} z$ terms, while NLL correspond to $\alpha_s^n \ln^{2n-4} z$, and NNLL to $\alpha_s^n \ln^{2n-5} z$. For $\hat{C}_{qg}^s(z)$ the corresponding power of $\ln z$ is lowered by 1. We have verified this general ansatz through explicit N³LO calculation. In Mellin space the corresponding ansatz reads

$$\begin{aligned} \mathcal{F}_{g/g}^{s(n)}(\bar{N}, \epsilon) &= \frac{1}{\epsilon^{2n-3}} \sum_{l=0}^{n-2} \frac{1}{\bar{N} - 2(n-1-l)\epsilon} (c_{gg}^{(1,l,n)} + \epsilon c_{gg}^{(2,l,n)} + \epsilon^2 c_{gg}^{(3,l,n)} + \dots), \\ \mathcal{F}_{q/g}^{s(n)}(\bar{N}, \epsilon) &= \frac{1}{\epsilon^{2n-4}} \sum_{l=0}^{n-3} \frac{1}{\bar{N} - 2(n-1-l)\epsilon} (c_{qg}^{(1,l,n)} + \epsilon c_{qg}^{(2,l,n)} + \epsilon^2 c_{qg}^{(3,l,n)} + \dots). \end{aligned} \quad (4.13)$$

Equations (4.13) and (4.9) provides the ansatz to resum all the large logarithms of z . On the right-hand side of Eq. (4.9), the ϵ expansion begins at order ϵ^{-n+1} for the n -loop contribution, and the non- ϵ^{-1} infrared poles are composed of lower-order coefficient functions and splitting functions, which can be regarded as known inputs. On the left-hand side of Eq. (4.9), for example, in the unfactorized function $\mathcal{F}_{g/g}^{s(n)}$, the ϵ series starts at order ϵ^{-2n+3} at n -loop as in Eq. (4.13). Expanding Eq. (4.9) up to ϵ^{-n+1} therefore yields $n-1$ linear equations which is sufficient to determine the $n-1$ unknown coefficients $c_{gg}^{(1,l,n)}$ with $l=0, \dots, n-2$. To reach NNLL accuracy, two additional powers of ϵ -expansion are required, that is, we need $\mathcal{F}_{g/g}^{s(n)}(\bar{N}, \epsilon)$ up to order ϵ^{-n+3} . A similar analysis shows that $\mathcal{F}_{q/g}^{s(n)}(\bar{N}, \epsilon)$ must be known up to order ϵ^{-n+3} in order to achieve NNLL accuracy. Of course, one may expand Eq. (4.9) further to ϵ^{-1} . The equations generated at this order enables the extraction of the splitting functions at the same perturbative order. Moreover, the resulting linear systems become over-determined, thereby providing a non-trivial consistency check for our resummation procedure. Finally, regarding to the solution of the DGLAP evolution equation Eq. (4.11), it can be showed that β_1 or higher-order coefficients of the beta function may safely be dropped, since they involve less divergent quantities in general.

In summary, the input for NNLL resummation are

$$\begin{aligned} &\beta_0, \\ &\gamma_0^T, \gamma_1^T, \gamma_2^T, \gamma_3^T, \\ &\mathcal{F}_{g(q)/g}^{s(0)} = 0, \mathcal{F}_{g(q)/g}^{s(1)} \text{ to } \epsilon^2, \mathcal{F}_{g(q)/g}^{s(2)} \text{ to } \epsilon^1, \mathcal{F}_{g(q)/g}^{s(3)} \text{ to } \epsilon^0. \end{aligned} \quad (4.14)$$

Following the approach outlined above, we obtain the resummed NNLL series truncated at order α_s^{15} , achieving a relative uncertainty below 0.1% up to $z \sim 10^{-3}$. The corresponding results are shown in Fig. 3, where we compare the fixed-order results with the resummed ones at different orders in α_s . Throughout, we set $N_f = 5$ for the number of light quark flavors. We observe that, even at N³LO, the effects of resummation remain important for $z < 10^{-2}$.

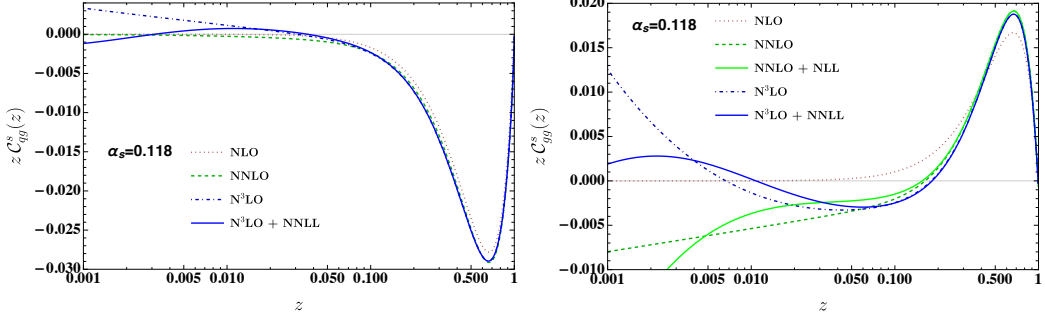


Figure 3. Coefficient functions for the linearly polarized gluon TMD FFs. The plots show the fixed-order results at NLO, NNLO and $N^3\text{LO}$, together with the resummed predictions including higher-order terms truncated at order α_s^{15} .

5 Conclusion

We have presented the $N^3\text{LO}$ twist-2 matching coefficients for linearly polarized gluon TMDs, together with the inclusion of next-to-next-to-leading logarithmic (NNLL) small- x resummation for the coefficient functions of gluon TMD fragmentation functions. The three-loop calculations were cross-checked in the $\mathcal{N} = 1$ supersymmetric limit, where the expected momentum sum rule was verified, providing a nontrivial consistency check of our results. Our results provide essential theoretical ingredients for forthcoming experiments such as the Electron–Ion Collider, which will probe the transverse momentum structure and polarization of gluons with unprecedented accuracy, and furnish fundamental small- x inputs for future studies of gluon dynamics and spin in high-energy QCD.

Acknowledgments

I thank Hua Xing Zhu for encouraging me to look into this problem and Tong-Zhi Yang for collaboration in the early stages of the project.

A QCD Beta Function

The QCD beta function is defined as

$$\frac{d\alpha_s}{d \ln \mu} = \beta(\alpha_s) = -2\alpha_s \sum_{n=0}^{\infty} \left(\frac{\alpha_s}{4\pi} \right)^{n+1} \beta_n, \quad (\text{A.1})$$

with [51]

$$\begin{aligned} \beta_0 &= \frac{11}{3}C_A - \frac{4}{3}T_F N_f, \\ \beta_1 &= \frac{34}{3}C_A^2 - \frac{20}{3}C_A T_F N_f - 4C_F T_F N_f, \\ \beta_2 &= \left(\frac{158C_A}{27} + \frac{44C_F}{9} \right) N_f^2 T_F^2 + \left(-\frac{205C_A C_F}{9} - \frac{1415C_A^2}{27} + 2C_F^2 \right) N_f T_F + \frac{2857C_A^3}{54}. \end{aligned} \quad (\text{A.2})$$

B Anomalous dimension

For all the anomalous dimensions entering the renormalization group equations of various TMD functions, we define the perturbative expansion in α_s according to

$$\gamma(\alpha_s) = \sum_{n=0}^{\infty} \left(\frac{\alpha_s}{4\pi} \right)^{n+1} \gamma_n, \quad (\text{B.1})$$

$$\begin{aligned}
\Gamma_0^{\text{cusp}} &= 4C_A, \\
\Gamma_1^{\text{cusp}} &= \left(\frac{268}{9} - 8\zeta_2 \right) C_A^2 - \frac{80C_A T_F N_f}{9}, \\
\Gamma_2^{\text{cusp}} &= \left[\left(\frac{320\zeta_2}{9} - \frac{224\zeta_3}{3} - \frac{1672}{27} \right) C_A^2 + \left(64\zeta_3 - \frac{220}{3} \right) C_F C_A \right] N_f T_F \\
&\quad + \left(-\frac{1072\zeta_2}{9} + \frac{88\zeta_3}{3} + 88\zeta_4 + \frac{490}{3} \right) C_A^3 - \frac{64}{27} C_A N_f^2 T_F^2, \\
\gamma_0^S &= 0, \\
\gamma_1^S &= \left[\left(-\frac{404}{27} + \frac{11\zeta_2}{3} + 14\zeta_3 \right) C_A + \left(\frac{112}{27} - \frac{4\zeta_2}{3} \right) T_F N_f \right] C_A, \\
\gamma_2^S &= \left(-\frac{88}{3} \zeta_3 \zeta_2 + \frac{6325\zeta_2}{81} + \frac{658\zeta_3}{3} - 88\zeta_4 - 96\zeta_5 - \frac{136781}{1458} \right) C_A^3 + \left(\frac{80\zeta_2}{27} - \frac{224\zeta_3}{27} \right. \\
&\quad \left. + \frac{4160}{729} \right) C_A N_f^2 T_F^2 + \left(-\frac{2828\zeta_2}{81} - \frac{728\zeta_3}{27} + 48\zeta_4 + \frac{11842}{729} \right) C_A^2 N_f T_F \\
&\quad + \left(-4\zeta_2 - \frac{304\zeta_3}{9} - 16\zeta_4 + \frac{1711}{27} \right) C_F C_A N_f T_F. \\
\gamma_0^R &= 0, \\
\gamma_1^R &= \left[\left(-\frac{404}{27} + 14\zeta_3 \right) C_A + \frac{112}{27} T_F N_f \right] C_A, \\
\gamma_2^R &= \left[\left(-\frac{824\zeta_2}{81} - \frac{904\zeta_3}{27} + \frac{20\zeta_4}{3} + \frac{62626}{729} \right) C_A N_f T_F + \left(-\frac{88}{3} \zeta_3 \zeta_2 + \frac{3196\zeta_2}{81} + \frac{6164\zeta_3}{27} \right. \right. \\
&\quad \left. \left. + \frac{77\zeta_4}{3} - 96\zeta_5 - \frac{297029}{1458} \right) C_A^2 + \left(-\frac{304\zeta_3}{9} - 16\zeta_4 + \frac{1711}{27} \right) C_F N_f T_F + \left(-\frac{64\zeta_3}{9} \right. \right. \\
&\quad \left. \left. - \frac{3712}{729} \right) N_f^2 T_F^2 \right] C_A. \quad (\text{B.2})
\end{aligned}$$

$$\begin{aligned}
\gamma_0^B &= \frac{11}{3} C_A - \frac{4}{3} T_F N_f, \\
\gamma_1^B &= C_A^2 \left(\frac{32}{3} + 12\zeta_3 \right) + \left(-\frac{16}{3} C_A - 4C_F \right) N_f T_F, \\
\gamma_2^B &= C_A^3 \left(-80\zeta_5 - 16\zeta_3 \zeta_2 + \frac{55}{3} \zeta_4 + \frac{536}{3} \zeta_3 + \frac{8}{3} \zeta_2 + \frac{79}{2} \right) \\
&\quad + C_A^2 N_f T_F \left(-\frac{20}{3} \zeta_4 - \frac{160}{3} \zeta_3 - \frac{16}{3} \zeta_2 - \frac{233}{9} \right) + \frac{58}{9} C_A N_f^2 T_F^2 - \frac{241}{9} C_A C_F N_f T_F
\end{aligned}$$

$$+2C_F^2N_fT_F+\frac{44}{9}C_FN_f^2T_F^2. \quad (\text{B.3})$$

The cusp anomalous dimension Γ^{cusp} can be found in [52]. The beam anomalous dimension γ^B is related to the soft anomalous dimension γ^S [53] and the hard anomalous dimensions γ^H [45, 54, 55] by renormalization group invariance condition $\gamma^B = \gamma^S - \gamma^H$. The rapidity anomalous dimension γ^R can be found in [37, 56]. Note that the normalization here differ from those in [37] by a factor of 1/2.

C Renormalization Constants

The following constants are needed for the renormalization of zero-bin subtracted [57] TMD PDFs through N³LO, see e.g. Ref. [27, 34]. The first three-order corrections to Z^B and Z^S are

$$\begin{aligned} Z_1^B &= \frac{1}{2\epsilon} (2\gamma_0^B - \Gamma_0^{\text{cusp}} L_Q) , \\ Z_2^B &= \frac{1}{8\epsilon^2} \left((\Gamma_0^{\text{cusp}} L_Q - 2\gamma_0^B)^2 + 2\beta_0(\Gamma_0^{\text{cusp}} L_Q - 2\gamma_0^B) \right) + \frac{1}{4\epsilon} (2\gamma_1^B - \Gamma_1^{\text{cusp}} L_Q) , \\ Z_3^B &= \frac{1}{48\epsilon^3} (2\gamma_0^B - \Gamma_0^{\text{cusp}} L_Q) \left(8\beta_0^2 + 6\beta_0 (-2\gamma_0^B + \Gamma_0^{\text{cusp}} L_Q) + (-2\gamma_0^B + \Gamma_0^{\text{cusp}} L_Q)^2 \right) \\ &\quad + \frac{1}{24\epsilon^2} \left(\beta_1 (-8\gamma_0^B + 4\Gamma_0^{\text{cusp}} L_Q) + (4\beta_0 - 6\gamma_0^B + 3\Gamma_0^{\text{cusp}} L_Q) (-2\gamma_1^B + \Gamma_1^{\text{cusp}} L_Q) \right) \\ &\quad + \frac{1}{6\epsilon} (2\gamma_2^B - \Gamma_2^{\text{cusp}} L_Q) \\ Z_1^S &= \frac{1}{\epsilon^2} \Gamma_0^{\text{cusp}} + \frac{1}{\epsilon} (-2\gamma_0^S - \Gamma_0^{\text{cusp}} L_\nu) , \\ Z_2^S &= \frac{1}{2\epsilon^4} (\Gamma_0^{\text{cusp}})^2 - \frac{1}{4\epsilon^3} \left(\Gamma_0^{\text{cusp}} (3\beta_0 + 8\gamma_0^S) + 4(\Gamma_0^{\text{cusp}})^2 L_\nu \right) - \frac{1}{2\epsilon} (2\gamma_1^S + \Gamma_1^{\text{cusp}} L_\nu) \\ &\quad + \frac{1}{4\epsilon^2} \left(\Gamma_1^{\text{cusp}} + 2(2\gamma_0^S + \Gamma_0^{\text{cusp}} L_\nu)(\beta_0 + 2\gamma_0^S + \Gamma_0^{\text{cusp}} L_\nu) \right) , \\ Z_3^S &= \frac{1}{6\epsilon^6} (\Gamma_0^{\text{cusp}})^3 - \frac{1}{4\epsilon^5} (\Gamma_0^{\text{cusp}})^2 (3\beta_0 + 4\gamma_0^S + 2\Gamma_0^{\text{cusp}} L_\nu) + \frac{1}{36\epsilon^4} \Gamma_0^{\text{cusp}} \left(22\beta_0^2 + 45\beta_0 (2\gamma_0^S + \Gamma_0^{\text{cusp}} L_\nu) \right. \\ &\quad \left. + 9(\Gamma_1^{\text{cusp}} + 2(2\gamma_0^S + \Gamma_0^{\text{cusp}} L_\nu)^2) \right) + \frac{1}{36\epsilon^3} \left(-16\beta_1 \Gamma_0^{\text{cusp}} - 12\beta_0^2 (2\gamma_0^S + \Gamma_0^{\text{cusp}} L_\nu) \right. \\ &\quad \left. - 2\beta_0 (5\Gamma_1^{\text{cusp}} + 9(2\gamma_0^S + \Gamma_0^{\text{cusp}} L_\nu)^2) - 3 \left[\Gamma_1^{\text{cusp}} (6\gamma_0^S + 9\Gamma_0^{\text{cusp}} L_\nu) \right. \right. \\ &\quad \left. \left. + 2 \left(8(\gamma_0^S)^3 + 6\Gamma_0^{\text{cusp}} \gamma_1^S + 12\Gamma_0^{\text{cusp}} (\gamma_0^S)^2 L_\nu + 6(\Gamma_0^{\text{cusp}})^2 \gamma_0^S L_\nu^2 + (\Gamma_0^{\text{cusp}})^3 L_\nu^3 \right) \right] \right) \\ &\quad + \frac{1}{18\epsilon^2} \left(2\Gamma_2^{\text{cusp}} + 3(2\beta_1 (2\gamma_0^S + \Gamma_0^{\text{cusp}} L_\nu) + (2\beta_0 + 6\gamma_0^S + 3\Gamma_0^{\text{cusp}} L_\nu) (2\gamma_1^S + \Gamma_1^{\text{cusp}} L_\nu)) \right) \\ &\quad - \frac{2\gamma_2^S + \Gamma_2^{\text{cusp}} L_\nu}{3\epsilon} . \quad (\text{C.1}) \end{aligned}$$

We remind the reader that the renormalization constants are formally identical for TMD PDFs and TMD FFs, the logarithms appeared above should be replaced by their corre-

sponding values in each case, and we have

$$L_{\perp} = \ln \frac{b_T^2 \mu^2}{b_0^2}, \quad L_{\nu} = \ln \frac{\nu^2}{\mu^2}, \quad (\text{C.2})$$

with $b_0 = 2 e^{-\gamma_E}$ for both TMD PDFs and TMD FFs.

For TMD PDFs,

$$L_Q = 2 \ln \frac{x P_+}{\nu}, \quad (\text{C.3})$$

while for TMD FFs,

$$L_Q = 2 \ln \frac{P_+}{z \nu}. \quad (\text{C.4})$$

References

- [1] P. M. Nadolsky, C. Balazs, E. L. Berger, and C. P. Yuan, *Gluon-gluon contributions to the production of continuum diphoton pairs at hadron colliders*, *Phys. Rev. D* **76** (2007) 013008, [[hep-ph/0702003](#)].
- [2] D. Boer, W. J. den Dunnen, C. Pisano, and M. Schlegel, *Determining the Higgs spin and parity in the diphoton decay channel*, *Phys. Rev. Lett.* **111** (2013), no. 3 032002, [[arXiv:1304.2654](#)].
- [3] F. Dominguez, J.-W. Qiu, B.-W. Xiao, and F. Yuan, *On the linearly polarized gluon distributions in the color dipole model*, *Phys. Rev. D* **85** (2012) 045003, [[arXiv:1109.6293](#)].
- [4] D. Boer, P. J. Mulders, J. Zhou, and Y.-j. Zhou, *Suppression of maximal linear gluon polarization in angular asymmetries*, *JHEP* **10** (2017) 196, [[arXiv:1702.08195](#)].
- [5] D. Boer, P. J. Mulders, and C. Pisano, *Dijet imbalance in hadronic collisions*, *Phys. Rev. D* **80** (2009) 094017, [[arXiv:0909.4652](#)].
- [6] D. Boer, S. J. Brodsky, P. J. Mulders, and C. Pisano, *Direct Probes of Linearly Polarized Gluons inside Unpolarized Hadrons*, *Phys. Rev. Lett.* **106** (2011) 132001, [[arXiv:1011.4225](#)].
- [7] D. Boer, P. J. Mulders, C. Pisano, and J. Zhou, *Asymmetries in Heavy Quark Pair and Dijet Production at an EIC*, *JHEP* **08** (2016) 001, [[arXiv:1605.07934](#)].
- [8] A. Efremov, N. Ivanov, and O. Teryaev, *How to measure the linear polarization of gluons in unpolarized proton using the heavy-quark pair leptoproduction*, *Phys. Lett. B* **777** (2018) 435–441, [[arXiv:1711.05221](#)].
- [9] C. Marquet, C. Roiesnel, and P. Taels, *Linearly polarized small- x gluons in forward heavy-quark pair production*, *Phys. Rev. D* **97** (2018), no. 1 014004, [[arXiv:1710.05698](#)].
- [10] A. Dumitru, T. Lappi, and V. Skokov, *Distribution of Linearly Polarized Gluons and Elliptic Azimuthal Anisotropy in Deep Inelastic Scattering Dijet Production at High Energy*, *Phys. Rev. Lett.* **115** (2015), no. 25 252301, [[arXiv:1508.04438](#)].
- [11] C. Pisano, D. Boer, S. J. Brodsky, M. G. Buffing, and P. J. Mulders, *Linear polarization of gluons and photons in unpolarized collider experiments*, *JHEP* **10** (2013) 024, [[arXiv:1307.3417](#)].

- [12] J.-P. Lansberg, C. Pisano, F. Scarpa, and M. Schlegel, *Pinning down the linearly-polarised gluons inside unpolarised protons using quarkonium-pair production at the LHC*, *Phys. Lett. B* **784** (2018) 217–222, [[arXiv:1710.01684](#)]. [Erratum: *Phys.Lett.B* 791, 420–421 (2019)].
- [13] A. Mukherjee and S. Rajesh, *Linearly polarized gluons in charmonium and bottomonium production in color octet model*, *Phys. Rev. D* **95** (2017), no. 3 034039, [[arXiv:1611.05974](#)].
- [14] U. D’Alesio, F. Murgia, C. Pisano, and P. Taels, *Azimuthal asymmetries in semi-inclusive $J/\psi + \text{jet}$ production at an EIC*, *Phys. Rev. D* **100** (2019), no. 9 094016, [[arXiv:1908.00446](#)].
- [15] A. Mukherjee and S. Rajesh, *J/ψ production in polarized and unpolarized ep collision and Sivers and $\cos 2\phi$ asymmetries*, *Eur. Phys. J. C* **77** (2017), no. 12 854, [[arXiv:1609.05596](#)].
- [16] J.-P. Lansberg, C. Pisano, and M. Schlegel, *Associated production of a dilepton and a $\Upsilon(J/\psi)$ at the LHC as a probe of gluon transverse momentum dependent distributions*, *Nucl. Phys. B* **920** (2017) 192–210, [[arXiv:1702.00305](#)].
- [17] R. Kishore and A. Mukherjee, *Accessing linearly polarized gluon distribution in J/ψ production at the electron-ion collider*, *Phys. Rev. D* **99** (2019), no. 5 054012, [[arXiv:1811.07495](#)].
- [18] D. Gutierrez-Reyes, S. Leal-Gomez, I. Scimemi, and A. Vladimirov, *Linearly polarized gluons at next-to-next-to leading order and the Higgs transverse momentum distribution*, *JHEP* **11** (2019) 121, [[arXiv:1907.03780](#)].
- [19] D. Boer, W. J. den Dunnen, C. Pisano, M. Schlegel, and W. Vogelsang, *Linearly Polarized Gluons and the Higgs Transverse Momentum Distribution*, *Phys. Rev. Lett.* **108** (2012) 032002, [[arXiv:1109.1444](#)].
- [20] M. G. Echevarria, T. Kasemets, P. J. Mulders, and C. Pisano, *QCD evolution of (un)polarized gluon TMDPDFs and the Higgs q_T -distribution*, *JHEP* **07** (2015) 158, [[arXiv:1502.05354](#)]. [Erratum: *JHEP* 05, 073 (2017)].
- [21] S. Catani and M. Grazzini, *QCD transverse-momentum resummation in gluon fusion processes*, *Nucl. Phys. B* **845** (2011) 297–323, [[arXiv:1011.3918](#)].
- [22] X. Chen, T. Gehrmann, E. W. N. Glover, A. Huss, Y. Li, D. Neill, M. Schulze, I. W. Stewart, and H. X. Zhu, *Precise QCD Description of the Higgs Boson Transverse Momentum Spectrum*, *Phys. Lett. B* **788** (2019) 425–430, [[arXiv:1805.00736](#)].
- [23] A. Gao, T.-Z. Yang, and X. Zhang, *The three-point energy correlator in the coplanar limit*, *JHEP* **08** (2025) 030, [[arXiv:2411.09428](#)].
- [24] M. A. Ebert, B. Mistlberger, and G. Vita, *TMD fragmentation functions at N^3LO* , *JHEP* **07** (2021) 121, [[arXiv:2012.07853](#)].
- [25] M. A. Ebert, B. Mistlberger, and G. Vita, *Transverse momentum dependent PDFs at N^3LO* , *JHEP* **09** (2020) 146, [[arXiv:2006.05329](#)].
- [26] M.-x. Luo, T.-Z. Yang, H. X. Zhu, and Y. J. Zhu, *Unpolarized Quark and Gluon TMD PDFs and FFs at N^3LO* , [arXiv:2012.03256](#).
- [27] M.-X. Luo, T.-Z. Yang, H. X. Zhu, and Y. J. Zhu, *Transverse Parton Distribution and Fragmentation Functions at NNLO: the Gluon Case*, *JHEP* **01** (2020) 040, [[arXiv:1909.13820](#)].

- [28] Y. Li, D. Neill, and H. X. Zhu, *An exponential regulator for rapidity divergences*, *Nucl. Phys. B* **960** (2020) 115193, [[arXiv:1604.00392](#)].
- [29] C. W. Bauer, S. Fleming, and M. E. Luke, *Summing Sudakov logarithms in $B \rightarrow X(s \gamma)$ in effective field theory*, *Phys. Rev. D* **63** (2000) 014006, [[hep-ph/0005275](#)].
- [30] C. W. Bauer, S. Fleming, D. Pirjol, and I. W. Stewart, *An Effective field theory for collinear and soft gluons: Heavy to light decays*, *Phys. Rev. D* **63** (2001) 114020, [[hep-ph/0011336](#)].
- [31] C. W. Bauer, D. Pirjol, and I. W. Stewart, *Soft collinear factorization in effective field theory*, *Phys. Rev. D* **65** (2002) 054022, [[hep-ph/0109045](#)].
- [32] C. W. Bauer, S. Fleming, D. Pirjol, I. Z. Rothstein, and I. W. Stewart, *Hard scattering factorization from effective field theory*, *Phys. Rev. D* **66** (2002) 014017, [[hep-ph/0202088](#)].
- [33] M. Beneke, A. Chapovsky, M. Diehl, and T. Feldmann, *Soft collinear effective theory and heavy to light currents beyond leading power*, *Nucl. Phys. B* **643** (2002) 431–476, [[hep-ph/0206152](#)].
- [34] M.-X. Luo, X. Wang, X. Xu, L. L. Yang, T.-Z. Yang, and H. X. Zhu, *Transverse Parton Distribution and Fragmentation Functions at NNLO: the Quark Case*, *JHEP* **10** (2019) 083, [[arXiv:1908.03831](#)].
- [35] M.-x. Luo, T.-Z. Yang, H. X. Zhu, and Y. J. Zhu, *Quark Transverse Parton Distribution at the Next-to-Next-to-Next-to-Leading Order*, *Phys. Rev. Lett.* **124** (2020), no. 9 092001, [[arXiv:1912.05778](#)].
- [36] J. Collins, *Foundations of perturbative QCD*, *Camb. Monogr. Part. Phys. Nucl. Phys. Cosmol.* **32** (2011) 1–624.
- [37] Y. Li and H. X. Zhu, *Bootstrapping Rapidity Anomalous Dimensions for Transverse-Momentum Resummation*, *Phys. Rev. Lett.* **118** (2017), no. 2 022004, [[arXiv:1604.01404](#)].
- [38] J.-y. Chiu, A. Jain, D. Neill, and I. Z. Rothstein, *The Rapidity Renormalization Group*, *Phys. Rev. Lett.* **108** (2012) 151601, [[arXiv:1104.0881](#)].
- [39] J.-Y. Chiu, A. Jain, D. Neill, and I. Z. Rothstein, *A Formalism for the Systematic Treatment of Rapidity Logarithms in Quantum Field Theory*, *JHEP* **05** (2012) 084, [[arXiv:1202.0814](#)].
- [40] S. Moch, B. Ruijl, T. Ueda, J. Vermaseren, and A. Vogt, *Four-Loop Non-Singlet Splitting Functions in the Planar Limit and Beyond*, *JHEP* **10** (2017) 041, [[arXiv:1707.08315](#)].
- [41] NNPDF Collaboration, R. D. Ball et al., *Parton distributions for the LHC Run II*, *JHEP* **04** (2015) 040, [[arXiv:1410.8849](#)].
- [42] S. Marzani, *Combining Q_T and small- x resummations*, *Phys. Rev. D* **93** (2016), no. 5 054047, [[arXiv:1511.06039](#)].
- [43] P. A. Baikov, K. G. Chetyrkin, A. V. Smirnov, V. A. Smirnov, and M. Steinhauser, *Quark and gluon form factors to three loops*, *Phys. Rev. Lett.* **102** (2009) 212002, [[arXiv:0902.3519](#)].
- [44] R. N. Lee, A. V. Smirnov, and V. A. Smirnov, *Analytic Results for Massless Three-Loop Form Factors*, *JHEP* **04** (2010) 020, [[arXiv:1001.2887](#)].
- [45] T. Gehrmann, E. Glover, T. Huber, N. Ikizlerli, and C. Studerus, *Calculation of the quark and gluon form factors to three loops in QCD*, *JHEP* **06** (2010) 094, [[arXiv:1004.3653](#)].

- [46] A. Vogt, *Resummation of small- x double logarithms in QCD: semi-inclusive electron-positron annihilation*, *JHEP* **10** (2011) 025, [[arXiv:1108.2993](#)].
- [47] H. Chen, T.-Z. Yang, H. X. Zhu, and Y. J. Zhu, *Analytic Continuation and Reciprocity Relation for Collinear Splitting in QCD*, [arXiv:2006.10534](#).
- [48] A. Mitov, S. Moch, and A. Vogt, *Next-to-Next-to-Leading Order Evolution of Non-Singlet Fragmentation Functions*, *Phys. Lett. B* **638** (2006) 61–67, [[hep-ph/0604053](#)].
- [49] S. Moch and A. Vogt, *On third-order timelike splitting functions and top-mediated Higgs decay into hadrons*, *Phys. Lett. B* **659** (2008) 290–296, [[arXiv:0709.3899](#)].
- [50] A. Almasy, S. Moch, and A. Vogt, *On the Next-to-Next-to-Leading Order Evolution of Flavour-Singlet Fragmentation Functions*, *Nucl. Phys. B* **854** (2012) 133–152, [[arXiv:1107.2263](#)].
- [51] P. Baikov, K. Chetyrkin, and J. Kühn, *Five-Loop Running of the QCD coupling constant*, *Phys. Rev. Lett.* **118** (2017), no. 8 082002, [[arXiv:1606.08659](#)].
- [52] S. Moch, J. Vermaseren, and A. Vogt, *The Three loop splitting functions in QCD: The Nonsinglet case*, *Nucl. Phys. B* **688** (2004) 101–134, [[hep-ph/0403192](#)].
- [53] Y. Li, A. von Manteuffel, R. M. Schabinger, and H. X. Zhu, *Soft-virtual corrections to Higgs production at $N^3\text{LO}$* , *Phys. Rev. D* **91** (2015) 036008, [[arXiv:1412.2771](#)].
- [54] S. Moch, J. Vermaseren, and A. Vogt, *Three-loop results for quark and gluon form-factors*, *Phys. Lett. B* **625** (2005) 245–252, [[hep-ph/0508055](#)].
- [55] T. Becher and M. Neubert, *On the Structure of Infrared Singularities of Gauge-Theory Amplitudes*, *JHEP* **06** (2009) 081, [[arXiv:0903.1126](#)]. [Erratum: JHEP 11, 024 (2013)].
- [56] A. A. Vladimirov, *Correspondence between Soft and Rapidity Anomalous Dimensions*, *Phys. Rev. Lett.* **118** (2017), no. 6 062001, [[arXiv:1610.05791](#)].
- [57] A. V. Manohar and I. W. Stewart, *The Zero-Bin and Mode Factorization in Quantum Field Theory*, *Phys. Rev. D* **76** (2007) 074002, [[hep-ph/0605001](#)].